Self-energy of zone-boundary phonons in germanium: *Ab initio* calculations versus neutron spin-echo measurements

J. Kulda,[1] A. Debernardi,[2] M. Cardona,[3] F. de Geuser,[1,*] and E. E. Haller[4]
[1]*Institut Laue-Langevin, B.P. 156, 38042 Grenoble Cedex 9, France*
[2]*INFM Democritos, UdR Trieste/SISSA, Strada Costiera 12, 34014 Trieste, Italy*
[3]*Max-Planck-Institut für Festkörperforschung, Heisenbergstrasse 1, D-70569, Stuttgart, Germany*
[4]*Department of Materials Science and Engineering, MC 1760, 210 Hearst Memorial Mining Building, University of California, Berkeley, California 94720, USA*

(Received 16 July 2003; revised manuscript received 24 September 2003; published 29 January 2004)

We present *ab initio* calculations and spin-echo measurements of the anharmonic self-energy of phonons at the *X* point of the Brillouin zone for germanium. The mechanisms that contribute to these self-energies are different from those usually displayed by phonons at the center of the Brillouin zone. Each mode shows trends representative of the variety of anharmonic mechanisms that are responsible for the scattering and the decay of phonons. The transverse acoustic phonons at the *X* point are very long lived at low temperatures; i.e., their probability of decay approaches zero, as a consequence of an unusual decay mechanism allowed by energy conservation. We have identified the microscopic processes that determine these self-energies. The calculated self-energies and their temperature dependence agree well with experiment.

DOI: 10.1103/PhysRevB.69.045209 PACS number(s): 78.70.Nx, 63.20.Ry, 31.15.Ar, 76.60.Lz

I. INTRODUCTION

The anharmonic self-energies of phonons in semiconductors have recently attracted considerable interest,[1–3] stimulated by *ab initio* calculations.[4–7] These self-energies determine two properties of collective excitations in the crystal which depend on the anharmonicity of the adiabatic interatomic potentials: the temperature (T) dependence of the frequencies of phonons and their lifetimes. The latter provide the main mechanism that governs the evolution of excited solids towards thermal equilibrium. As an effect of anharmonic interaction, a nonequilibrium phonon population (created either by the annihilation of hot carriers or by electromagnetic radiation) decays into phonons of lower energy or is scattered by thermal phonons into modes of different frequencies. For these reasons the phonon self-energies have been the subject of many experimental studies.[8] The poor resolution achieved with conventional inelastic neutron scattering (INS), however, has restricted such work mainly to first-order Raman spectroscopy, to which only phonons close to the center of the Brillouin zone (BZ) are accessible. Developments in the neutron spin-echo (NSE) technique[9,10] have recently opened the way to more accurate determinations of the real and imaginary parts of the phonon self-energies at other points in the BZ.

Here we report calculated (*ab initio*) and measured (by NSE) self-energies at the *X* point of the BZ for isotopically pure germanium. The calculated real part agrees with NSE results as well as with data obtained by INS.[11] Agreement between the calculated imaginary part and the neutron spin-echo data is excellent. Each of the three phonon modes at *X* exhibits different decay mechanisms that originate in anharmonic processes which are more varied than those displayed by the BZ center phonons investigated up to date. We show that in germanium a nonequilibrium transverse acoustic (TA) phonon population at the X-point is rather stable at low temperature. The trends of anharmonic decay processes for the transverse optical (TO) and acoustic (TA) phonons as well as for the degenerate longitudinal modes (LA and LO) are discussed. We analyze the microscopic processes involved in the decay and scattering of these phonons. The results lead to guidelines for the anharmonic behavior of similar, hitherto uninvestigated phonons in other tetrahedral semiconductors.

II. PHONON SELF-ENERGY

Phonons in an isotopically pure harmonic crystal are noninteracting and live forever.[12] Phonon-phonon interactions originate from crystal anharmonicity that is characterized by the phonon self-energy, $\Delta(\omega)-i\Gamma(\omega)$.[13] For a phonon of peak frequency Ω the real part $\Delta(\Omega)$ represents the frequency shift due to scattering and is responsible for the temperature dependence of Ω. The probability of phonon decay, described by $\Gamma(\Omega)$, determines the phonon lifetime ($\tau^{-1}=2\Gamma$). It can be measured in time-resolved Raman experiments[14,15] or obtained from the linewidth measured by Raman spectroscopy[8,16] (equal to 2Γ if the peak displays a Lorentzian line shape). Here we use equivalently both terms, lifetime and linewidth [i.e., 2Γ is the full width at half maximum (FWHM) of the experimental peak], to describe the imaginary part of the self-energy. To the lowest order in the expansion of the total energy E_{tot} with respect to the mode amplitude $\mathbf{e}_j$ (eigenvector of the harmonic Hamiltonian) the width of a phonon of frequency ω and wave vector $\mathbf{q}$ in the jth branch is[17]

$$\Gamma_j(\mathbf{q};\omega)=\frac{\pi}{2\hbar^2}\sum_{\mathbf{G},\mathbf{q}_1,\mathbf{q}_2,j_1,j_2}\left|\frac{\partial^3 E_{\mathrm{tot}}}{\partial\mathbf{e}_j(\mathbf{q})\partial\mathbf{e}_{j_1}(\mathbf{q}_1)\partial\mathbf{e}_{j_2}(\mathbf{q}_2)}\right|^2 \times\delta(-\mathbf{q}+\mathbf{q}_1+\mathbf{q}_2+\mathbf{G})\{[n_{j_1}(\mathbf{q}_1)+n_{j_2}(\mathbf{q}_2)+1] \times\delta(\omega-\omega_{j_1}(\mathbf{q}_1)-\omega_{j_2}(\mathbf{q}_2))+2[n_{j_1}(\mathbf{q}_1)-n_{j_2}(\mathbf{q}_2)] \times\delta(\omega+\omega_{j_1}(\mathbf{q}_1)-\omega_{j_2}(\mathbf{q}_2))\}, \quad (1)$$

where **G** is a reciprocal lattice vector and $n_j(\mathbf{q})$ is the Bose-Einstein factor of the jth phonon mode with wave vector **q** and harmonic frequency ω_j. The first term within $\{\cdots\}$ on the right-hand side of Eq. (1) is responsible for the decay into two phonons of lower energy (*downconversion* or *sum processes*); the second term for the processes in which a nonequilibrium phonon with a thermal phonon are destroyed while a phonon of higher energy is created (*upconversion*[14] or *difference processes*).

The real part of the self-energy is composed of three contributions $\Delta_j(\mathbf{q};\omega)=\Delta_j^{(0)}(\mathbf{q})+\Delta_j^{(3)}(\mathbf{q};\omega)+\Delta_j^{(4)}(\mathbf{q})$. The term $\Delta_j^{(0)}(\mathbf{q})$ corresponds to the change in frequency due to thermal expansion (the so-called quasiharmonic approximation); $\Delta_j^{(3)}(\mathbf{q};\omega)$ represents three-phonon decay processes, and it is obtained through the Hilbert transform of $\Gamma_j(\mathbf{q};\omega)$ (we call it the third order term); $\Delta_j^{(4)}(\mathbf{q})$ is related to the fourth derivative of the total energy and represents the shift of the phonon frequency due to elastic scattering by one thermal phonon (the fourth order term). The frequency Ω_j that includes the anharmonic contributions is the solution of a Dyson equation; in the usual case of small $\Delta_j(\omega)$ it can be simplified to $\Omega_j=\omega_j+\Delta_j(\Omega_j)$. The temperature dependence of Δ and Γ is computed by density functional perturbation theory[6] and plane-wave pseudopotential techniques.[18,19] The anharmonic force constants are obtained as described in Ref. 7. We use a plane-wave expansion of the electronic density with a kinetic energy cutoff of 20 Ry and an 888-point grid[20–22] for **q**-space integration.

III. EXPERIMENTAL TECHNIQUE

Our experiments have been performed using the spin-echo option TASSE (Ref. 9) on the IN20 polarized neutron three-axis spectrometer at the Institut Laue-Langevin in Grenoble. The sample was a single crystal of about 5 cm^3, Czochralski grown from material enriched to 96.8% of the ^{74}Ge isotope. This high isotopic purity eliminates phonon scattering due to mass disorder.[15] The spectrometer was operated with a fixed final neutron wave number $k_f=4.1$ Å^{-1}. The exact position of the [0, 0, 0.8] TA mode to be investigated was placed in the [3, 3, 1] BZ by conventional $Q=$const scans with precession fields off. Next, the spectrometer was kept at a fixed configuration corresponding to the maximum of the phonon peak at $Q=[3, 3, 1.8]$ with an energy transfer of $\Delta E=9.8$ meV so that only currents in the coils of the spin-echo setup have been driven in the rest of the experiment.

The NSE technique[10] employs the Larmor precession to precisely measure small changes in energy of each neutron upon scattering in the sample. The variation of the mean energy transfer ΔE is reflected by the shift of the spin-echo phase, $\Delta\varphi=\tau_F\Delta E/\hbar$, where τ_F is the Fourier time, a parameter characterizing the sensitivity of the given instrument configuration. It is proportional to the field integral in the coils and to the cube of the neutron wavelength. A finite intrinsic width of an excitation line introduces an additional energy spread into the scattered neutrons, resulting in an enhanced precession phase spread and hence in stronger damping of the echo amplitude. We have used two measurement

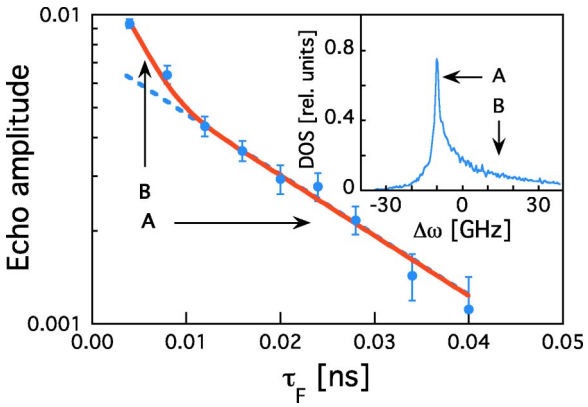

FIG. 1. (Color online) The spin-echo amplitude as a function of the Fourier time at $T=280$ K. The inset displays the calculated density of TA phonon states within the resolution volume of the IN20 NSE setup. The letters *A* and *B* label its narrow and broad components, respectively, and point to the corresponding slopes in the main part.

modes. First, recording a sequence of spin-echo scans at various Fourier times, but at otherwise unchanged conditions, permitted to deduce the intrinsic linewidth [i.e., $2\Gamma(\Omega)$] from the damping of the echo signal. Second, recording the spin-echo phase variations as a function of temperature at a fixed Fourier time, optimally chosen on the basis of the preceding linewidth measurements, we have followed the thermal variation of the excitation energy [i.e., $\Delta(\Omega)$].

A typical spin-echo amplitude versus τ_F is shown in Fig. 1. If the line profile were described by a Lorentzian, an exponential damping would be observed. The more complicated dependence observed suggests that the real profile is more complicated. A histogram in the inset of Fig. 1 displays the distribution of frequencies of the investigated TA mode corresponding to **q** vectors lying within the resolution volume. Indeed, in addition to the almost singular component corresponding to the chosen flat part of the dispersion branch, there is a broad shoulder corresponding to points on the periphery of the resolution volume. Although the integral weight of this broad part is even higher than that of the narrow central peak, the two components can be resolved in the Fourier spectrum thanks to the difference in their widths. As the IN20 spin-echo setup does not permit measurements at $\tau_F<0.002$ ns to characterize the broad component and, as the calculations themselves have estimative power only (the ''broad'' component still represents an energy spread below 1% of the nominal excitation energy), we have assumed a tail of a Gaussian profile having an FWHM of 73 GHz and a fixed amplitude ratio to the Lorentzian part to provide an adequate representation of this effect.

IV. RESULTS AND DISCUSSION

We report data for the self-energy of germanium phonons at or near the X point of the BZ. The experimental data refer to the $(0,0,0.8)2\pi/a_L$ point of the conventional cell of side a_L, while the computation was performed for the X point

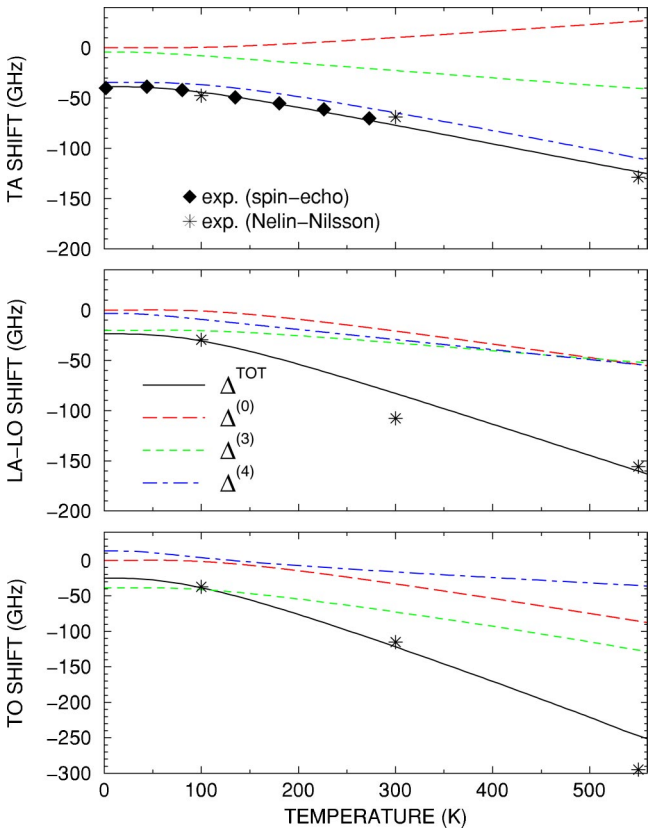

FIG. 2. (Color online) $\Delta(\mathbf{X};\Omega)$ of germanium vs temperature. Diamonds: NSE measurements. Stars: INS experimental data from Ref. 11. Solid lines: *ab initio* results. The low-order contributions to the real part of the self-energy are displayed as dotted, dashed, or dot-dashed lines.

$(0,0,1)2\pi/a_L$ (Ref. 23). In Fig. 2 we display the real part of the phonon self-energy versus temperature. The results of the calculations for the three lowest-order contributions are also shown, added up (Δ^{TOT}, solid line) and compared with measurements by spin-echo (diamonds) or INS (stars).[11] The calculations yield absolute values for zero temperature whereas the measurements yield only the shift with respect to the renormalized frequency for $T=0$. We have therefore shifted the experimental data by the self-energy calculated for absolute zero.[24] As displayed in Fig. 2, the contribution to the shift due to the thermal expansion ($\Delta^{(0)}$) is positive for the TA mode, whereas it is negative for the other modes (the TO contribution is roughly twice the LA-LO one), reflecting the sign and magnitude of the corresponding mode Grüneisen parameters. For TA modes this positive contribution is added to the negative ones of third and fourth order, resulting in a small temperature dependence of the phonon frequency.

According to Fig. 2, at absolute zero, $\Delta^{(4)}$ is negative for the TA mode, it is almost negligible for LA-LO, and small and positive for the TO modes; this follows from the fact that each mode weighs differently the positive and negative contributions associated with the scattering of the *X* phonon by either optical or acoustic modes: generally the former is positive while the latter is negative. At room temperature, when acoustic modes become thermally populated, $\Delta^{(4)}$ is negative for all the modes under consideration. For the TA mode $\Delta^{(3)}$ is much smaller than $\Delta^{(4)}$, while the opposite is true for the TO mode. For the latter (the highest-frequency mode among those investigated here), the low-order anharmonic terms display a behavior similar to that already noticed for BZ center modes in most of the III-V semiconductors,[6] while they become progressively different as the frequency of the mode under investigation (LO-LA and TA) decreases. These regular trends suggest that our results for phonons at *X* are representative of the different anharmonic mechanisms responsible for scattering and decay of phonons of nonvanishing wave vector in tetrahedral semiconductors. The computed real part of the self-energy agrees well with experiment, also at high temperature where higher-order terms neglected here are expected to be important.

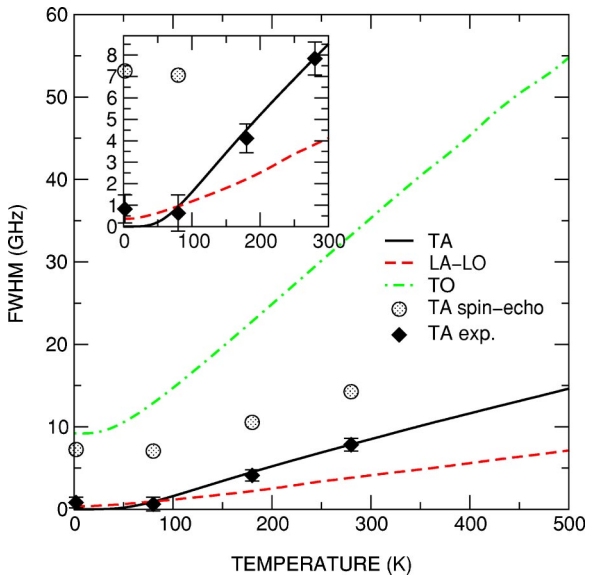

FIG. 3. (Color online) $2\Gamma(\mathbf{X};\Omega)$ of germanium vs temperature. Diamonds: experimental results for TA phonons when spurious contributions are subtracted. Circles: the original spin-echo measurements. *Ab initio* data are displayed as the solid line (TA mode), dashed line (LO-LA modes), and dot-dashed line (TO mode).

In the main panel of Fig. 3 we display the decay probabilities $2\Gamma(\Omega)$ (FWHM) vs *T* over the whole temperature range investigated, while in the inset we report our data for the modes of lower FWHM up to 300 K. The first important consequence of Fig. 3 is that the $2\Gamma_{\mathrm{TA}}(\Omega)$ nearly vanishes at absolute zero: the phonon is long lived and its lifetime is not likely to be related to anharmonic components of the potential energy but to other mechanisms.[25] The vanishing of the decay probability when the temperature tends to zero reflects the absence of thermal phonon population. Here the only microscopic process allowed by energy conservation is the decay into acoustic phonons of lower energy whose wave vector is close to the BZ center. Not only is the density of final states small for such processes, but as a consequence of translational symmetry, the corresponding matrix elements must vanish for $\mathbf{q}\rightarrow 0$.[26] According to our calculations, for TA phonons the downconversion contribution remains negligible in the entire range of temperatures studied. The only significant contributions arise from upconversion processes; this also explains the narrow linewidths (less than the experi-

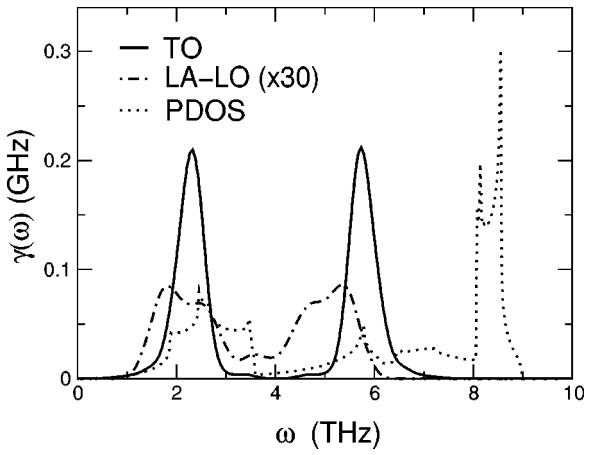

FIG. 4. Solid and dot-dashed lines: frequency-resolved final-state spectrum $\gamma(\omega)$ calculated for LA-LO (multiplied by 30) and TO modes at the X point in germanium at absolute zero. Dotted line: one-phonon density of states (arbitrary units).

mental resolution) measured by INS.[11]

The decay of the TO phonons, on the contrary, is almost entirely governed by downconversion processes, as has also been found for center-zone phonons. As noticed during the discussion of $\Delta(\Omega)$, the LA(LO) mode is an ''intermediate case'' between the TO and TA: both upconversion and downconversion processes contribute to the temperature dependence of the decay probability (at 300 K they are of the same size); however, the combined effects remain smaller than for the TA phonons except below 80 K. We explain these trends with the *frequency-resolved final-state spectrum*[4] $\gamma(\omega)$ displayed in Fig. 4 for the LA-LO and TO modes at $T=0$ [at absolute zero $\gamma_{\mathrm{TA}}(\omega)=0$] together with the one-phonon density of states (PDOS). $\gamma(\omega)$ is the probability per unit time that the phonon decays into one mode of frequency ω, the frequency of the other mode given by energy conservation,[27] by definition, $2\Gamma=\int d\omega\,\gamma(\omega)$, and the peaks of $\gamma(\omega)$ are placed symmetrically around one-half of the frequency of the decaying mode. At $T=0$ only the downconversion processes are active. $\gamma_{\mathrm{TO}}(\omega)$ is mainly determined by processes that involve decay into a TA and an LA(LO) phonon: the main peaks correspond to frequencies of large PDOS (the peak at $\sim$5.8 THz coincides with a van Hove singularity). On the contrary, $\gamma_{\mathrm{LA\text{-}LO}}$ (magnified in the figure) is very small because the allowed decay processes are not supported by a significant density of final states. For this reason, the downconversion contribution of this mode remains small also at higher temperature. At finite temperature the upconversion mechanism becomes active. The corresponding process destroys the LA-(LO) phonon at X together with a thermal acoustic one and creates a phonon in the optical branches; energy conservation constrains the thermal phonon to a frequency in a region of very low PDOS, and the decay probability of the LA(LO) modes remains rather small even at 500 K. Energy conservation allows upconversion of the TA mode into an optical mode of higher frequency by destroying mainly thermal phonons in the K-W region of the BZ, where there is a singularity in the PDOS. For this reason $\Gamma_{\mathrm{TA}}(\mathbf{X})$ becomes larger than $\Gamma_{\mathrm{LA(LO)}}(\mathbf{X})$ as soon as the temperature populates the phonon states that are to be destroyed in the upconversion process. This situation differs radically from that found for the optical mode at the BZ center where only the downconversion mechanism is significant.[4,6]

V. CONCLUSIONS

We have presented experimental and theoretical results for the self-energy of phonon modes of germanium at the X point of the BZ. The mechanisms that contribute to the self-energy of TO modes are similar to those previously found for zone-center phonons of tetrahedral semiconductors whereas the decay of the TA modes is related to anharmonic processes that are different from those of the TO modes. At low temperature this mode has a long lifetime corresponding to the vanishing of decay probability for $T\rightarrow 0$. Trends of the self-energy have been discussed in detail in terms of microscopic mechanisms responsible for the decay and scattering processes. The upconversion process is also dominant for the low E_2 mode of wurtzite semiconductors.[28] This mode can be regarded as a TA mode folded from the edge of the BZ of zinc-blende structure. We conjecture that the results presented here may also shed light upon the corresponding modes of other tetrahedral semiconductors (i.e., those with zinc-blende, wurtzite, or chalcopyrite structures) for which no information is available.

Note added in proof. After the completion of our work we have noticed the publication of a paper by G. Deinzer *et al.*,[29] in which the imaginary part of phonon self-energy in Si and Ge is computed by the method employed in Refs. 6, 12. In order to compute the temperature dependent phonon line widths, Deinzer *et al.* approximate the frequency of the decaying mode by its zero-temperature harmonic value, while in the present study the frequencies of the X-phonon modes are taken consistently weith the computed thermal shifts displayed in Fig. 2, which include the temperature dependent anharmonic contributions.

ACKNOWLEDGMENTS

We thank the Istituto Nazionale per la Fisica della Materia for the ''Iniziativa Trasversale di Calcolo Parallelo.'' M.C. would like to acknowledge support from the Fonds der Chemischen Industrie.

*Present address: Groupe de Physique des Materiaux UMR CNRS 6634, Université de Rouen, Rouen, France.

[1] F.J. Manjón, J. Serrano, I. Loa, K. Syassen, C.T. Lin, and M. Cardona, Phys. Rev. B **64**, 064301 (2001).

[2] A. Debernardi, C. Ulrich, K. Syassen, and M. Cardona, Phys. Rev. B **59**, 6774 (1999).

[3] C. Ulrich, E. Anastassakis, K. Syassen, A. Debernardi, and M. Cardona, Phys. Rev. Lett. **78**, 1283 (1997).

[4] A. Debernardi, S. Baroni, and E. Molinari, Phys. Rev. Lett. **75**, 1819 (1995).

[5] A. Debernardi and M. Cardona, Physica B **263**, 687 (1999).

[6] A. Debernardi, Phys. Rev. B **57**, 12 847 (1998).

[7] A. Debernardi, Solid State Commun. **113**, 1 (2000).
[8] J. Menéndez and M. Cardona, Phys. Rev. B **29**, 2051 (1984).
[9] C.M.E. Zeyen, J. Phys. Chem. Solids **60**, 1573 (1999).
[10] J. Kulda, E. Farhi, and C.M.E. Zeyen, Physica B **316–317**, 383 (2002).
[11] G. Nelin and G. Nilsson, Phys. Rev. B **10**, 612 (1974).
[12] See, e.g., N.W. Ashcroft and N.D. Mermin, *Solid State Physics* (Holt-Sanders, Tokyo, 1981).
[13] R.A. Cowley, J. Phys. (Paris) **26**, 659 (1965).
[14] F. Vallée, Phys. Rev. B **49**, 2460 (1994).
[15] H.D. Fuchs, C.H. Grein, R.I. Devlen, J. Kuhl, and M. Cardona, Phys. Rev. B **44**, 8633 (1991).
[16] B.A. Weinstein, Solid State Commun. **20**, 999 (1976).
[17] A. Debernardi, Physica B **316–317**, 35 (2002).
[18] D.R. Hamann, M. Schluter, and C. Chiang, Phys. Rev. Lett. **43**, 1494 (1979).
[19] G.B. Bachelet, R. Hamann, and M. Schluter, Phys. Rev. B **26**, 4199 (1982).
[20] H.J. Monkhorst and J.D. Pack, Phys. Rev. B **13**, 5188 (1976).
[21] D.J. Chadi and M.L. Cohen, Phys. Rev. B **8**, 5747 (1973).
[22] D.J. Chadi, Phys. Rev. B **16**, 1746 (1977).
[23] Germanium has the crystal structure of diamond fcc with two atoms per primitive cell. We use a cell with a reduced symmetry containing four germanium atoms: the phonon at X are folded back into the center of the BZ.
[24] The widths in Fig. 3 represent the damping of the echo signal corresponding to the narrow Lorentzian component at Fourier times in the range between 0.012 and 0.04 ns. Here 6.5 GHz have been subtracted from the observed values. This component includes the instrumental resolution, the spread due to dispersion (within the narrow peak in the inset of Fig. 1), and the contribution of phonon damping by crystal defects and mass disorder.
[25] T. Klitsner and R.O. Pohl, Phys. Rev. B **36**, 6551 (1987).
[26] For a general proof see Ref. 6, Appendix B.
[27] $\gamma(\omega)$ is computed inserting in Eq. (1) a normalized Gaussian $\propto \exp\{[\omega-\omega_j(\mathbf{q})]^2/2\sigma\}$ with $\sigma \simeq 0.15$ THz.
[28] J. Serrano, F.J. Manjón, A.H. Romero, F. Widulle, R. Lauck, and M. Cardona, Phys. Rev. Lett. **90**, 055510 (2003).
[29] G. Deinzer, G. Birner, and D. Strauch, Phys. Rev. B **67**, 144304 (2003).